J|A|C|S ARTICLES

Published on Web 01/08/2010

Presentation of Membrane-Anchored Glycosphingolipids Determined from Molecular Dynamics Simulations and NMR Paramagnetic Relaxation Rate Enhancement

Mari L. DeMarco, Robert J. Woods,* James H. Prestegard, and Fang Tian*,†

Complex Carbohydrate Research Center, University of Georgia, 315 Riverbend Road, Athens, Georgia 30602

Received September 4, 2009; E-mail: rwoods@ccrc.uga.edu; ftian@psu.edu

Abstract: Challenges for structural characterization of membrane-bound glycosphingolipids include their high internal dynamic motions and their physical proximity to membrane surfaces. Here we demonstrate that NMR paramagnetic relaxation enhancement can be used, alongside independent molecular dynamics simulations and an outer-sphere relaxation model, to quantitatively characterize the presentation (insertion depth and orientation relative to a membrane surface) of ganglioside GM1 in biologically relevant membrane environments. Longitudinal and transverse paramagnetic relaxation enhancement effects were measured for GM1, anchored to phospholipid bicelles, using both water-soluble and membrane-anchored paramagnetic probes, respectively. A method was developed to rapidly calculate paramagnetic relaxation enhancement effects from thousands of structures taken from a simulation of GM1 in a phospholipid bilayer. The combined computational and experimental approach yielded experimentally verified atomic-resolution 3D models of a highly plastic membrane-bound biomolecule.

Introduction

Membrane-bound glycosphingolipids (GSLs) are involved in many critical biological processes, including cell adhesion and signal transduction.[1] Their primary location, in the outer-leaflet of the plasma membrane, also makes them targets for invading pathogens attempting to adhere to host cells.[2−4] To gain a better understanding of these cell-surface interactions, characterization of the 3D structure of membrane-bound GSLs is required; however, their high internal plasticity and physical proximity to membrane surfaces makes structural characterization in biologically relevant environments challenging. Additionally, current experimental methods to characterize 3D structure of glycolipids do not include *presentation* effects (insertion depth and orientation relative to a membrane surface) in their analysis. Previous NMR studies of GSLs have explored: (1) residue composition, anomeric configuration and linkage information via chemical shifts and *J*-coupling constants;[5,6] (2) internal 3D structure via inter-residue nuclear Overhauser enhancements (NOEs);[7] and (3) orientation relative to the plane of the membrane surface via residual dipolar couplings.[8] More recently, paramagnetic relaxation enhancement (PRE) from NMR spectroscopy has emerged as a powerful tool for the structural characterization of biomolecules, including the identification of solvent-exposed protein surfaces[9,10] and mapping the orientation of micelle-bound peptides with various paramagnetic agents.[11−13] In the current study, we developed PRE experiments and models to explore presentation effects of a representative GSL, β-Gal-(1−3)-β-GalNAc-(1−4)-[α-Neu5Ac-(2−3)]-β-Gal-(1−4)-β-Glc-(1−1)-ceramide (GM1) (Figure 1). PRE data from NMR experiments on bicelle-anchored GM1, along with an independent all-atom explicit solvent molecular dynamics (MD) simulation of GM1 in a phospholipid bilayer were used to probe both the 3D structure and presentation of a membrane-bound GSL.

Materials and Methods

Materials. Gd(III)-diethylenetriamine pentaacetic acid (Gd-(DTPA)), 5-doxyl stearic acid (5-DSA), 3-([3-cholamidopropyl]-dimethylammonio)-2-hydroxy-1-propanesulfonate (CHAPSO) and monosialoganglioside GM1 from bovine brain were purchased from Sigma. 1,2-Dimyristoyl-*sn*-glycero-3-phosphocholine (DMPC) was obtained from Avanti Polar Lipids. Deuterium oxide was purchased from Cambridge Isotope Lab.

Sample Preparations and NMR Spectroscopy. A stock bicelle solution was prepared with 78 mg DMPC, 145 mg CHAPSO and

† Current address: Department of Biochemistry and Molecular Biology, Penn State College of Medicine, 500 University Dr., Hershey, PA 17033.

(1) Degroote, S.; Wolthoorn, J.; van Meer, G. *Semin. Cell Dev. Biol.* **2004**, *15*, 375.
(2) Eidels, L.; Proia, R. L.; Hart, D. A. *Microbiol. Rev.* **1983**, *47*, 596–620.
(3) Hug, P.; Lin, H. M.; Korte, T.; Xiao, X.; Dimitrov, D. S.; Wang, J. M.; Puri, A.; Blumenthal, R. *J. Virol.* **2000**, *74*, 6377–85.
(4) Suzuki, Y. *Prog. Lipid Res.* **1994**, *33*, 429.
(5) Koerner, T. A. W.; Prestegard, J. H.; Demou, P. C.; Yu, R. K. *Biochemistry* **2002**, *22*, 2676.
(6) Koerner, T. A. W.; Prestegard, J. H.; Demou, P. C.; Yu, R. K. *Biochemistry* **2002**, *22*, 2687.
(7) Acquotti, D.; Poppe, L.; Dabrowski, J.; Vonderlieth, C. W.; Sonnino, S.; Tettamanti, G. *J. Am. Chem. Soc.* **1990**, *112*, 7772–7778.
(8) Aubin, Y.; Ito, Y.; Paulson, J. C.; Prestegard, J. H. *Biochemistry* **1993**, *32*, 13405–13413.
(9) Pintacuda, G.; Otting, G. *J. Am. Chem. Soc.* **2002**, *124*, 372–373.
(10) Hernandez, G.; Teng, C.-L.; Bryant, R. G.; LeMaster, D. M. *J. Am. Chem. Soc.* **2002**, *124*, 4463.
(11) Respondek, M.; Madl, T.; Gobl, C.; Golser, R.; Zangger, K. *J. Am. Chem. Soc.* **2007**, *129*, 5228–5234.
(12) Al-Abdul-Wahid, M. S.; Neale, C.; Pomes, R.; Prosser, R. S. *J. Am. Chem. Soc.* **2009**, *131*, 6452.
(13) Papavoine, C. H. M.; Konings, R. N. H.; Hilbers, C. W.; van de Ven, F. J. M. *Biochemistry* **2002**, *33*, 12990.

 10.1021/ja907518x

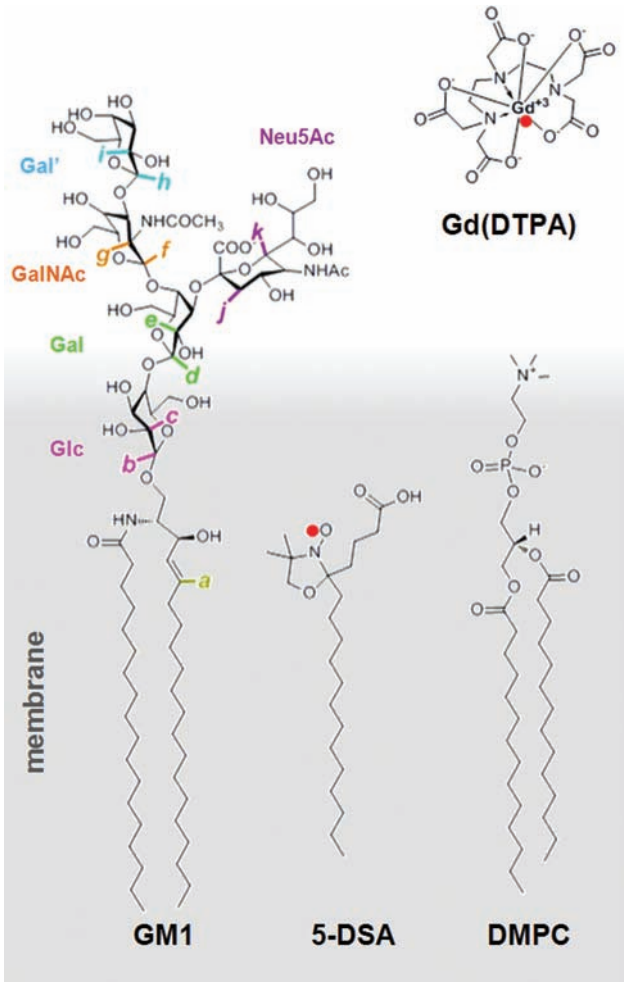

Figure 1. Molecules of interest: GM1 (with key protons labeled *a*−*k*), DMPC, and the paramagnetic probes 5-DSA and Gd(DTPA).

1 mL of 20 mM phosphate, pH 7.5 D_2O solution (molar ration of DMPC to CHAPSO = 0.5). Samples with 1 mg GM1 in 280 mL of bicelle stock solution in a 4 mm regular NMR tube were used for NMR experiments. For the measurements of PREs, the Gd(DTPA) was titrated to a final concentration of 1.5 mM from a stock solution of 200 mM Gd(DTPA) and 330 mM EDTA. The NMR sample for a membrane soluble PRE probe had 3.2 mM 5-DSA. All NMR spectra were acquired at 42 °C on a Varian 900 MHz spectrometer equipped with gradient triple resonance cold probe. The acquisition parameters are provided in the Supporting Information.

MD Simulations. Two all-atom explicit solvent 20 ns simulations were run using the AMBER 9 version of PMEMD:[14] (1) GM1 in a DMPC bilayer, and (2) the carbohydrate fragment of GM1 (*β*-Gal-(1−3)-*β*-GalNAc-(1−4)-[α-Neu5Ac-(2−3)]-*β*-Gal-(1−4)-*β*-Glc-(1−1)-OH) in solution. The simulations were run using the TIP3P water model and GLYCAM06 parameters for DMPC, GM1 and the GM1-fragment.[15−17] (full details of system setup and equilibration are given in the Supporting Information). Subsequent analyses were performed at 10 ps intervals: PRE calculations (Table 1), proton−proton distances (Table 2), and accessible surfaces (Table 3 and S1 of the Supporting Information). Ramachandran-style density plots of the glycosidic torsion

Table 1. Paramagnetic Relaxation Rate Enhancements, R^{pre}, of GM1 in the Presence of the Solution Probe Gd(DTPA) and the Membrane-Bound Probe 5-DSA, As Measured from NMR Experiment and As Calculated Using Snapshots from the MD Trajectory

		R_1^{pre} with Gd(DTPA) (s^{-1})		R_2^{pre} with 5-DSA (s^{-1})
protons	residue	NMR	MD	NMR
a	Cer	0.12 ± 0.03	0.044 ± 0.01	17 ± 2
b	Glc	0.21 ± 0.04	0.081 ± 0.02	3.7 ± 3
c	Glc	0.20 ± 0.04	0.082 ± 0.02	11 ± 4
d	Gal	0.28 ± 0.01	0.15 ± 0.03	0.85 ± 0.6
e	Gal	0.24 ± 0.03	0.23 ± 0.04	0.78 ± 1
f	GalNAc	0.41 ± 0.02	0.40 ± 0.07	0.28 ± 1
g	GalNAc	0.33 ± 0.03	0.36 ± 0.06	−0.31 ± 1
h	Gal′	0.86 ± 0.02	0.82 ± 0.1	0.16 ± 0.8
i	Gal′	0.80 ± 0.02	0.97 ± 0.3	0.028 ± 0.4
j	Neu5Ac	0.63 ± 0.05	0.59 ± 0.2	0.85 ± 0.6
k	Neu5Ac	0.63 ± 0.02	0.55 ± 0.1	0.67 ± 2

populations (Figure S2 of the Supporting Information) were calculated at 1 ps intervals.

The NACCESS program[18] was used to compute accessible surface areas (ASA), using a 1.4 and 4.5 Å probe radius to mimic water and Gd(DTPA), respectively. To obtain a reference value for each glycosyl residue, ensemble average ASAs (<ASA>) were calculated by averaging the results for individual snapshots from the simulation of the carbohydrate fragment of GM1 (Table S1 of the Supporting Information). The <ASA> of the glycosyl residues from GM1 in the lipid bilayer were also determined (Table S1 of the Supporting Information) and were reported as a percent of the average values for the carbohydrate fragment in solution (Table 3).

PRE Model. To quantitatively interpret PREs by a freely diffusing Gd(DTPA) probe, an outer-sphere relaxation model was employed.[11] In this model, the molecular diffusion is considered to be frozen on the time scale of the fast electron relaxation and the PRE of a nucleus is simply approximated by the sum of its relaxation enhancements from each of the paramagnetic centers. The longitudinal relaxation rate enhancement in the presence of a paramagnetic probe, R_1^{pre} is as follows:

$$R_1^{pre} = \sum_i \frac{2}{15}\left(\frac{\mu_0}{4\pi}\right)^2 \frac{\gamma_I^2 (g_J \mu_B)^2 J(J+1)}{r_i^6}\left(\frac{3\tau_c}{1+\omega_H^2\tau_c^2} + \frac{7\tau_c}{1+\omega_S^2\tau_c^2}\right) \quad (1)$$

where the symbols have their usual meaning. r_i represents a distance between the nucleus and the i^{th} paramagnetic probe. For protons of GM1, $R_1^{pre}$was predicted from MD snapshots taken at 10 ps granularity from the 20 ns simulation of GM1 embedded in a DMPC bilayer. To model the diffusion of the water-soluble paramagnetic probe Gd(DTPA), a grid was created (at 1 Å spacing), about GM1 and the DMPC bilayer, indicating possible populations of the probe (Figure 2). The 3D grid extended 25 Å from any GM1 atom. We tested larger grids but found that PRE effects from outside this region were negligible. Any grid point whose van der Waals radius, $r_{Gd(DTPA)} = 4.5$ Å, overlapped with that of a DMPC or GM1 atom was excluded. The radius of Gd(DTPA) was approximated from the van der Waals volume of the molecule. For each sterically allowed grid point within 25 Å of GM1 and the lipid bilayer, the rate was calculated with eq 1 (assuming a single correlation time for all protons) and then scaled by its occupancy. The probability of Gd(DTPA) occupying each grid point was defined by the concentration of the paramagnetic agent and scaled by the Boltzmann distribution factors calculated from the potential energy of

(14) Case, D. A.; Cheatham, T. E., 3rd; Darden, T.; Gohlke, H.; Luo, R.; Merz, K. M., Jr.; Onufriev, A.; Simmerling, C.; Wang, B.; Woods, R. J. *J. Comput. Chem.* **2005**, *26*, 1668–88.
(15) Kirschner, K. N.; Yongye, A. B.; Tschampel, S. M.; González-Outeiriño, J.; Daniels, C. R.; Foley, B. L.; Woods, R. J. *J. Comput. Chem.* **2008**, *29*, 622–655.
(16) Tessier, M. B.; DeMarco, M. L.; Yongye, A.; Woods, R. J. *Mol. Simul.* **2008**, *34*, 349–364.
(17) DeMarco, M. L.; Woods, R. J. *Glycobiology* **2009**, *19*, 344–355.
(18) Hubbard, S. J.; Thornton, J. M.; *Department of Biochemistry and Molecular Biology*, University College of London: London, 1993.

Table 2. Proton−Proton Distances (Å) Calculated from MD Simulations, Compared with Experimental Intra- and Inter-residue NOE Distances for GM1 in Solution and GM1-Modified Micelles[a]

proton−proton contacts		MD[b]	NMR experiment[c]		crystal structures[f]	
		GM1 in DMPC bilayer	GM1-acetyl micelles[d]	GM1 in DMSO[e]	3chb (chain E)	3bwr (chain A)
Gal′−H1	GalNAc−H2	4.2 ± 0.4	3.0 ± 0.3	3.5 ± 0.4	4.1	4.3
Gal′−H1	GalNAc−H3	2.4 ± 0.3		2.5 ± 0.3	2.3	2.1
Gal′−H1	GalNAc−H2N	3.5 ± 0.7	3.0 ± 0.3	2.5 ± 0.4	3.4	3.9
Neu5Ac−H8O	Neu5Ac−H6	3.3 ± 0.7	2.2 ± 0.2	2.4 ± 0.2	2.0	2.1
Neu5Ac−H8	GalNAc−H1	4.7 ± 1.9		3.1 ± 0.3	2.3	2.7
Neu5Ac−H8O	GalNAc−H1	6.0 ± 2.2	2.9 ± 0.3	2.6 ± 0.3	2.5	2.5
Neu5Ac−H3A	Gal−H3	3.0 ± 1.0	2.4 ± 0.2		2.2	2.1
Neu5Ac−H3A	Gal−H2O	3.2 ± 0.5	3.4 ± 0.3	3.2 ± 0.3	2.6	2.5
GalNAc−H2N	GalNAc−H2	2.6 ± 0.2	2.5 ± 0.3	2.6 ± 0.3	2.4	2.3
GalNAc−H2N	Gal−H2	3.9 ± 0.6	3.4 ± 0.3	3.6 ± 0.4	3.8	3.9
GalNAc−H1	Gal−H4	2.3 ± 0.2	2.4 ± 0.2	2.2 ± 0.2	2.1	2.0
Gal−H2O	Glc−H61	4.1 ± 0.9		3.6 ± 0.4	5.4	7.1
Gal−H2O	Glc−H62	3.3 ± 0.5		3.4 ± 0.3	3.7	5.7
Gal−H1	Glc−H3O	3.5 ± 0.8		3.5 ± 0.4	3.8	2.5
Gal−H1	Glc−H6O	4.8 ± 1.3		>4	4.7	5.4

[a] For qualitative comparison, the proton−proton distances of the pentasaccharide fragment of GM1 bound to proteins shown in Figure 6, are also given. [b] Ensemble average proton−proton distances, with standard deviations reported. [c] Experimental error was estimated at 10%.[24] [d] Data from GM1-micelles where the ceramide of GM1 has been replaced with an acetyl group.[21] [e] Data from GM1 monomers in a solution of DMSO.[7] [f] Hydrogens were added, then energy minimized for 100 steps (holding non-hydrogen atoms fixed).

Table 3. Changes in the Accessibility of the Carbohydrate Epitope when Membrane Bound[a]

residue	relative ASA of GM3 (%)	relative ASA of GM1 (%)	
	water[17]	water	Gd(DTPA)
Glc	27 ± 10	25 ± 10	1.7 ± 3
Gal	73 ± 10	34 ± 10	2.2 ± 6
GalNAc		81 ± 8	46 ± 10
Gal′		96 ± 7	85 ± 10
Neu5Ac	95 ± 5	84 ± 10	43 ± 10

[a] The relative ASA (%) values for the glycosyl residues of GM3 (α-Neu5Ac-(2−3)-β-Gal-(1−4)-β-Glc-Cer) and GM1 are relative to the <ASA> calculated for the same residues from the simulation of the associated carbohydrate fragment of the GSL in solution.

charge−charge interactions between Gd(DTPA) and GM1, and the screening effect of salt, using a Columbic potential energy function. The PRE for each proton of interest was then obtained by summing the probability-weighted PRE at each grid point. A single correlation time (1 ns) was used for all protons; however, this number became arbitrary as a scaling factor was then used, and accounts for potential uncertainties in the variables included in the calculation (correlation times, concentrations, etc).[19] The calculated PREs were empirically scaled according to the set of experimental values by attempting to maximize a correlation coefficient with slope of the regression line equal to one.

Results and Discussion

NMR Data Collection. The overwhelming signals from DMPC and CHAPSO in our samples preclude direct observations of GM1 resonances. We employed the 2D selective TOCSY experiment with a zero quantum filter[20] to suppress lipid resonances and to resolve overlapped GM1 resonances (Figure 3a). For Glc, Gal, GalNAc, and Gal′, the experiment selectively built the connection of the H2 proton to the anomeric resonance (H1). For the measurements of longitudinal relaxation rates, the selective 2D TOCSY sequence was preceded by a nonselective 180° pulse and a recovery delay. For the measurements of transverse relaxation rates (R_2^{pre}), the delay τ was varied. Figure 3, parts (b) and (c) are examples of selective 2D TOCSY spectra of GM1. The fast tumbling of the bicelles and the mobility of GM1 yielded high resolution spectra with resonance line-widths of several hertz. The diffusion rates for DMPC and GM1 were similar, confirming the anchoring of GM1 to the bicelles (data not shown). In Figure 3b, although H1 protons of GM1 (*b*, *d*, and *h* in Figure 1) overlapped with other resonances, the relaxation rates could be measured precisely from their cross-peaks to H2 protons (*c*, *e*, and *i*, respectively). Similarly, although H2 protons (*c*, *e*, and *i*) are buried in lipid resonances, their relaxation rates could be measured precisely from their cross-peaks to H1 protons (*b*, *d*, and *h*, respectively) (Figure 3c).

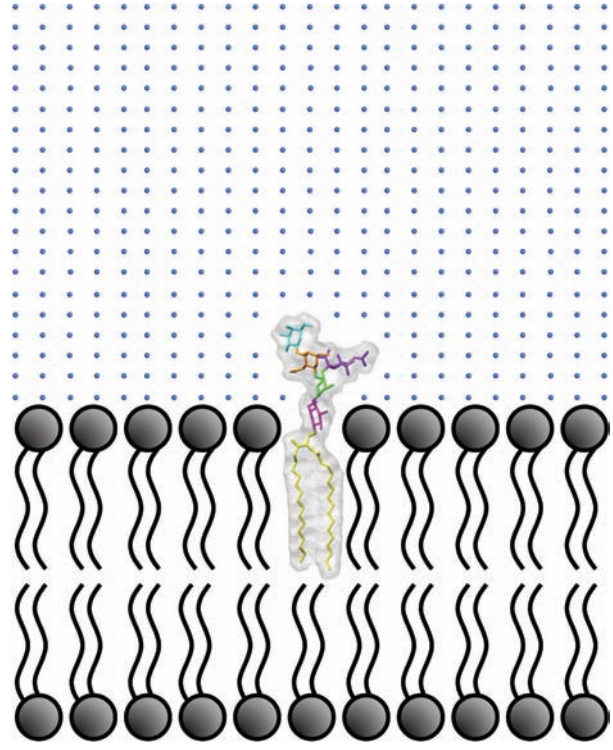

Figure 2. A model for calculating PREs from MD snapshots. The diffusion of the water-soluble paramagnetic probe Gd(DTPA) was modeled using a grid (blue dots), and the probability of the probe being at each grid point was included in the PRE calculation. For clarity, here we show the lipids as cartoons, but in the calculation all-atom MD snapshots (containing DMPC molecules, with the waters removed), were used.

(19) Clore, G. M.; Iwahara, J. *Chem. Rev.* **2009**, *109*, 4108–4139.
(20) Thrippleton, M. J.; Keeler, J. *Angew. Chem., Int. Ed. Engl.* **2003**, *42*, 3938–3941.

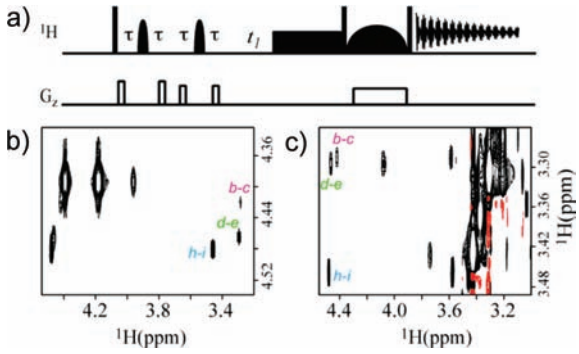

Figure 3. (a) The pulse sequence for selective 2D TOCSY experiment with a zero quantum filter. Parts (b) and (c) are example spectra acquired with a g3 selective inversion pulses with a bandwidth of 440 Hz at 4.58 ppm and with a g3 selective inversion pulses with a bandwidth of 200 Hz at 4.379 ppm, respectively. The TOCSY mixing time was 30 ms.

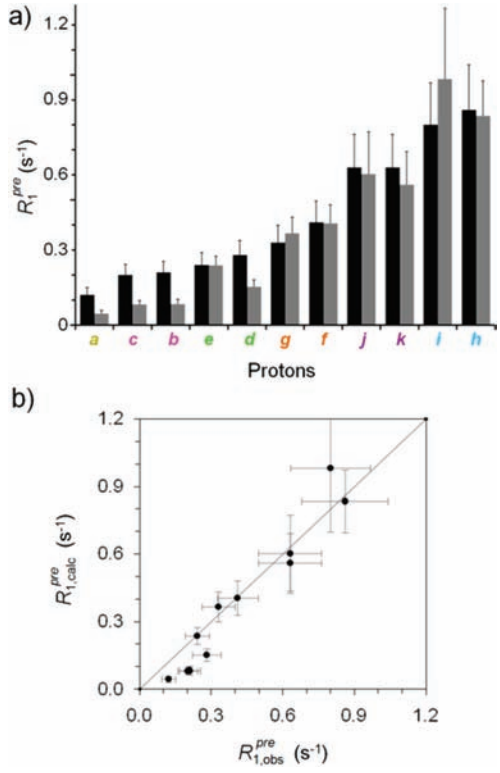

Figure 4. PREs using the Gd(DTPA) probe, as observed via NMR ($R_{1,obs}^{pre}$) and calculated using MD snapshots ($R_{1,calc}^{pre}$) for GM1 protons (see Figure 1). (a) Gradation of the PRE effect: $R_{1,obs}^{pre}$ (black bars, with error bars) are shown in order of increasing magnitude, and $R_{1,calc}^{pre}$ (gray bars, with standard deviations) represent an ensemble of 2000 structures from the MD simulation (b) Correlation between $R_{1,obs}^{pre}$ and $R_{1,calc}^{pre}$.

A water-soluble probe, Gd(DTPA) was chosen for PRE measurements since the negatively charged paramagnetic complex was unlikely to interact with the negatively charged GM1, CHAPSO, or phosphate carrying lipids (Figure 1). The absence of specific interactions with GM1 was evidenced by the negligible perturbation of the GM1 spectra in the presence of Gd(DTPA). In addition, PRE experiments were conducted using the membrane-bound probe 5-DSA (Figure 1). With two selective 1D and three selective 2D TOCSY experiments, we were able to detect two protons from each carbohydrate residue and a methylene proton from the ceramide portion of GM1 and determined their longitudinal and transverse PRE rates in the presence of the water-soluble and membrane-bound probe,

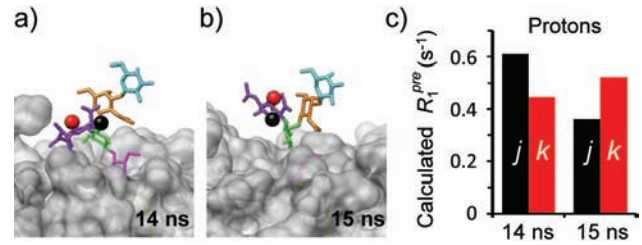

Figure 5. PREs calculated from MD snapshots, based on the Gd(DTPA) probe model, are sensitive to changes in the conformation of the GSL and its presentation relative to the membrane surface (gray). Part (a) 14 ns and (b) 15 ns snapshots from MD (shown perpendicular to bilayer normal with protons *j* and *k* as spheres), and (c) their corresponding calculated PRE effect.

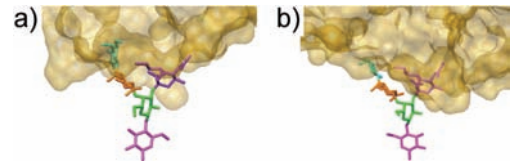

Figure 6. Consistent with PRE results and MD simulations, pathogenic proteins (gold) recognize cell-surface GM1 through interactions with Gal′ (cyan) and Neu5Ac (purple). Crystal structures of (a) cholera toxin (3CHB chain E) and, (b) VP1 (3BWR, chain A), solved with the carbohydrate fragment of GM1.

respectively (Table 1). Qualitatively, these results were consistent with our model of membrane-anchored GM1. Protons in/near the membrane had larger PRE effects from the membrane soluble probe, 5-DSA and smaller effects from the water-soluble probe, Gd(DTPA), while protons which were further away from the membrane showed smaller PRE effects from the membrane soluble probe, 5-DSA and large effects from the water-soluble probe, Gd(DTPA).

Internal 3D Structure of GM1. Prior to using the MD-predicted ensemble of GM1/DMPC bilayer structures for calculating PRE effects using our method, we validate the predicted conformational space sampled by GM1 over the course of the MD simulation using available experimental NOE data from GM1 in solution and GM1-acetyl micelles.[7,21] Ensemble average proton−proton distances derived from the MD simulation were in statistical agreement with experimentally derived NOE distances, with the exception of one from the acetyl group of Neu5Ac (Table 2). During the simulation the acetyl group of Neu5Ac did repeatedly form conformers consistent with the NOE distance; however, since the experimentally derived NOE distances were for GM1-acetyl micelles and monomeric GM1 in DMSO, it is not possible to determine if the MD simulation under-sampled the dominant acetyl conformer observed experimentally, or if anchoring intact GM1 to a phospholipid membrane slightly alters the relative populations. Importantly, the conformation of the Neu5Ac−Gal glycosidic linkage was in accord with the NOE data, based on proton−proton distances from ring-protons of Neu5Ac to Gal and no calculated PREs involved protons from the acetyl group of Neu5Ac. The remaining distances were all consistent with the experimental data (Table 2).

Presentation Effects. In addition to internal 3D conformation, structural characterization of GSLs in biologically relevant environments requires analysis of presentation effects relative to the membrane surface. Our experimentally observed PREs

(21) Brocca, P.; Berthault, P.; Sonnino, S. *Biophys. J.* **1998**, *74*, 309–318.

provided long-range structural markers of presentation that qualitatively agreed with a static model. However, we sought to quantitatively interpret this data and relate it to the conformational ensemble populated by membrane-anchored GM1. To this end, we used snapshots from the GM1/DMPC MD simulation to calculate average longitudinal relaxation rate enhancements experienced by protons from the ensemble of membrane-bound structures (details in the Methods section) (Figure 4a). As has been shown previously, an empirical scaling factor was derived to optimize the computed set of PREs against the experimental data set,[19] which resulted in a correlation coefficient of 0.9 between the observed and calculated data sets (Figure 4b).

While the accessibility of GSL protons to the paramagnetic probe is explicitly included in our PRE model, we also computed changes in ASA to provide an additional quantitative measure of the presentation of GM1 with respect to the membrane surface (Table 3). These results were compared with our previous 30 ns MD simulation of a related GSL, GM3 (α-Neu5Ac-(2−3)-β-Gal-(1−4)-β-Glc-Cer), where the insertion depth and orientation of known protein binding epitopes of the GSL were experimentally validated.[17] GM3, like GM1, displayed similar trends in solvent accessibility upon anchoring to a membrane (Table 3). From the MD snapshots and subsequent ASA calculations, we found that the ceramide had expectedly low accessible surface area over the course of the simulation. Residues Glc and Gal were also shielded from solvent (Table 3), due to the proximity of hydrophilic phosphocholine groups of neighboring DMPC molecules. This surface occlusion accounted for the small PREs from the water-soluble probe observed and computed for protons from Cer, Glc, and Gal (Figure 4a). For protons further from the plane of the membrane (based on MD simulations), and hence more accessible to the paramagnetic agent Gd(DTPA), larger PRE perturbations were measured (Figure 4a).

To complement the Gd(DTPA) data, PRE measurements from the membrane-anchored probe 5-DSA showed the opposite sensitivities: protons from ceramide, and Glc were the only protons to experience significant PRE effects (Table 1). Protons from the remainder of the carbohydrate domain had little or no statistically significant relaxation enhancements (Table 1), consistent with MD results showing that these protons reside at or above the membrane surface.

While the long-range distance constraints provided by NMR using paramagnetic probes are powerful structural measurements, it should be kept in mind that for flexible molecules experimental PREs represent the average PRE experienced by a proton from an ensemble of structures, with no direct means to then identify the individual conformational populations that constitute that ensemble. However, NMR complemented by unbiased MD simulations (no NMR restraints) provides a means to explore the multiple conformers and the fluctuating local membrane-environments that give rise to the ensemble data. Our code was designed to rapidly calculate PREs for thousands of PDB files so that analysis of a MD trajectory was possible. This aim avoided the need to select for representative low-energy conformers and allowed for extensive sampling of lipid molecule positioning relative to the GSL (which effects presentation of the GSL and hence PRE effects). For instance, given two snapshots from the MD trajectory (Figure 5), we have shown how PRE measurements are sensitive to conformational changes of the GSL and positional changes in the lipid environment. Additionally, information on the dynamics of the system can be obtained by using an ensemble of structures for PRE calculations. For example, Gal′ and Neu5Ac had the largest standard deviations of the calculated PREs (Figure 4), which was a reflection of the large conformational heterogeneity of their glycosidic linkages (Figure S2, parts a and c, of the Supporting Information), relative to conformational space populated by the other glycosidic angles. It is, in part, this dynamic behavior that contributed to fluctuations in the accessibility of the probe.

From the standpoint of cell-surface molecular recognition, our results are consistent with the carbohydrate binding epitopes of proteins known to bind GM1 at the plasma membrane surface. In the PDB there are structures of two proteins known to bind GM1 at membrane surfaces, solved with the pentasaccharide fragment of GM1. One belongs to the family of bacterial enterotoxins, cholera toxin secreted by *V. cholera*, and the other is a viral capsid protein, VP1 from Simian virus 40.[22,23] Both cholera toxin (PDB ID: 3CHB) and VP1 (PDB ID: 3BWR) bind the pentasaccharide fragment of GM1 primarily through interactions with Gal′ and Neu5Ac (Figure 6).[22,23] These binding epitopes are consistent with both observed and calculated PRE effects for membrane-bound GM1, whereby Gal′ and Neu5Ac protons experienced the greatest PRE effects in the presence of the water-soluble probe (Figure 4a). The PRE data also account for why these pathogenic proteins may have evolved to recognize discontinuous epitopes; because they are the most accessible surfaces of the GSL, as viewed by an extracellular protein attempting to adhere to a host cell.

Conclusions

Our studies have demonstrated that PREs from NMR can be understood in a reasonably quantitative way by developing a method that can rapidly calculate PREs from thousands of objectively generated 3D structures. We have shown, using highly plastic membrane-bound GSL, that PREs capture changes in internal conformation, membrane insertion depth, and orientation, which lead to changes in the presentation of the binding epitopes of cell surface molecules. Most notably, MD simulations used in combination with NMR PRE data can be used to translate sparse structural data into experimentally verified atomic-resolution 3D models of highly plastic membrane-bound biomolecules.

Acknowledgment. We are grateful for financial support from the National Institutes of Health (RR05351, 5R01GM081793-03) and the Georgia Research Alliance (GRA.VAC09.J).

Supporting Information Available: Detailed NMR and MD methods, and additional results including example longitudinal relaxation data (with and without the water-soluble probe) and Ramachandran-style plots of the glycosidic torsion angles populated during the simulation. This material is available free of charge via the Internet at http://pubs.acs.org. The program used for PRE calculations is available upon request from the authors.

JA907518X

(22) Merritt, E. A.; Kuhn, P.; Sarfaty, S.; Erbe, J. L.; Holmes, R. K.; Hol, W. G. J. *J. Mol. Biol.* **1998**, *282*, 1043.
(23) Neu, U.; Woellner, K.; Gauglitz, G.; Stehle, T. *Proc. Natl. Acad. Sci. U. S. A.* **2008**, *105*, 5219–5224.
(24) Keepers, J. W.; James, T. L. *J. Magn. Reson.* **1984**, *57*, 404–426.